INTERNATIONAL ELECTRONIC JOURNAL OF GEOMETRY
VOLUME 17 NO. 2 PAGE 336–347 (2024)
DOI: HTTPS://DOI.ORG/10.36890/IEJG.1318186

The Intersection Curve of an Hyperbolic Cylinder with a Torus Sharing the Same Center

Ana Maria Reis D'Azevedo Breda*, Alexandre Emanuel Batista da Silva Trocado and José Manuel Dos Santos Dos Santos

(Communicated by Kazım İlarslan)

ABSTRACT

This work aims to classify the families of curves obtained by the intersection of an arbitrary hyperbolic cylinder with an arbitrary torus sharing the same center, based on the number of their connected components and the number of their self-intersections points. The graphic geometric representation of these curves, in GeoGebra, and the respective algebraic descriptions, supported from a theoretical and computational point of view, are of fundamental importance for the development of this work. In this paper, we describe the procedure and the necessary implementation to achieve the outlined objective.

Keywords: *GeoGebra, toric sections, quadrics, intersection curves.*

AMS Subject Classification (2020): *Primary: 00A69 ; Secondary: 14H50; 14J29; 14Q05; 14Q10.*

1. Introduction

The development of the Constructive Solid Geometry (CSG) method is of great importance in solid modeling. The CSG method includes the combination of two basic three-dimensional shapes (rectangular prism, cylinder, cone, sphere, and torus) by means of three Boolean operations, namely, the *join* (union), the *cut* (difference), and the *intersect* (intersection). In [5], Ku-Jin Kim and Myung-Soo Kim, presents an efficient and robust geometric algorithm that classifies and detects all possible types of torus/sphere intersections, including all degenerate conic sections (circles) and singular intersections.

Our interest is to study, from a geometric, algebraic, and topological point of view, the intersection curve of a torus with a hyperbolic cylinder that shares the same center [2]. As we shall see, this curve can take a variety of shapes depending on the parameters of the torus and the hyperbolic cylinder. What we can surely say is that it is a closed curve with 4-fold symmetry.

The study we set out to carry out is interesting not only from a mathematical point of view for the detection of curves with interesting topological properties and from the point of view of modeling 3D shapes but also from the point of view of other areas, for example, physics in the description of the geometry of toroidal magnetic confinement devices such as tokamaks [6].

Based on methods described for studying intersection curves from a geometric, algebraic, and topological point of view [2], and considering the complexity of classifying these curves in the general case, the study focused, initially, on the classification of intersection curves of a torus with an ellipsoid sharing the same center, based on the number of connected components and the number of their self-intersection points [1]. Here, the quadric in consideration is a hyperbolic cylinder. The method used is supported by the subresultant theorem for multivariate polynomials [8], applying this result to the intersection of two quadrics using the GeoGebra [7] and also Maple [3, 4] software.

Received : 22-07-2023, Accepted : 07-01-2024
** Corresponding author*

In the next sections, we will use the same terminology used in [1],[2].

2. The surfaces

Let $\mathcal{T}$ be a torus centred at the origin, O, of the Cartesian coordinate system and with axis along the z-axis. Denoting the radius from the center of the hole to the center of the torus tube by rM and the radius of the tube by rm, where $rM > rm$, $\mathcal{T}$ can be described by the algebraic equation:

$$\mathcal{T}_{(O,rM,rm)} : (x^2 + y^2 + z^2 + rM^2 - rm^2)^2 - 4\,rM^2\,(x^2 + y^2) = 0. \tag{2.1}$$

Let us, now, consider a hyperbolic cylinder, $\mathcal{H}$, centred at $O = (0, 0, 0)$.

Aiming at the classification of the intersection curves of $\mathcal{T}$ with $\mathcal{H}$, we will consider, separately, the following two cases.

- $\mathcal{H}$ is a hyperbolic cylinder with axis along the z-axis.

$$\mathcal{H}_{(a,b)} : \frac{x^2}{a^2} - \frac{y^2}{b^2} - 1 = 0. \tag{2.2}$$

  with a and b, two positive real numbers.

- $\mathcal{H}$ is a hyperbolic cylinder along an axis lying in the plane xOy.
  Observe that, in this case, we may assume, without loss of generality, that $\mathcal{H}$ is a hyperbolic cylinder along the x-axis. Thus, $\mathcal{H}$ can be described by the equation,

$$\mathcal{H}_{(b,c)} : \frac{y^2}{b^2} - \frac{z^2}{c^2} - 1 = 0. \tag{2.3}$$

  with b and c, two positive real numbers.

3. Algorithm

The procedure employed, in both cases, make use of the following steps:

1. Compute the squarefree polynomial $\mathbf{S}_0(x, y)$, corresponding to the **resultant** of the two surface polynomial equations, in order to z.

2. Describe the admissible region $\mathcal{A}$, which is a region bounded by the projection of the two surface in xOy, containing the cutcurve (part of the curve $\mathbf{S}_0$ in $\mathcal{A}$), that is, containing the projection in xOy of the intersection curve of the two surfaces;

3. Compute the critical points of the curve $\mathbf{S}_0(x, y) = 0$ (roots of $\mathbf{Resultant}(\mathbf{S}_0(x, y), \frac{\partial \mathbf{S}_0}{\partial y}(x, y); y)$), and detect the singular points;

4. Compute the regular points of the curve $\mathbf{S}_0(x, y) = 0$ in the critical lines. The lifting of these regular points is performed by using the implicit Torus or Quadric equation.

5. Compute the points of the cutcurve in the silhouette curves. These points will never be lifted.

6. Use the previously computed information to determine the topology of the curve.

7. Compute the branches of the cutcurve (inside $\mathcal{A}_{\mathcal{E}_1,\mathcal{E}_2}$) by using closed formulae involving radicals.

8. Obtain the intersection curve of the two considered surfaces by lifting the branches of the cutcurve using parametric equations of the torus (see [2]).

4. The case $\mathcal{T}\bigcap\mathcal{H}_{(a,b)}$

The projection of (the curve) $\mathcal{T}\bigcap\mathcal{H}_{(a,b)}$ in the xOy plane is given by the squarefree polynomial:

$$S_0 = a^2y^2 - x^2b^2 + a^2b^2.$$

The cutcurve is contained within the region delimited by two circles and is defined by

$$(rM - rm)^2 \leq x^2 + y^2 \leq (rM + rm)^2.$$

The cardinality of the intersection points of the cutcurve with the boundary of the admissible region is either 0, 2, or 4. In case of intersection, these points are given by:

$$\left(\pm\sqrt{\frac{(rM-rm)^2+b^2}{a^2+b^2}}\,a, \pm\sqrt{\frac{(rM-rm)^2-a^2}{a^2+b^2}}\,b\right).$$

Regarding the intersection points of the cutcurve with the outer circle, their coordinates are given by:

$$\left(\pm\sqrt{\frac{(rM+rm)^2+b^2}{a^2+b^2}}\,a, \pm\sqrt{\frac{(rM+rm)^2-a^2}{a^2+b^2}}\,b\right).$$

Table 1 presents a succinct summary of the conditions governing the variation of the parameters a and b, covering all cases.

	$0 < b < \infty$	$b \to +\infty$	$b \to 0$
$a < rM - rm$	4 connected components (Figure 1a)	4 connected components (Figure 1b)	4 connected components (Figure 1c)
$a = rM - rm$	2 connected components with 2 self-intersection points (Figure 2a)	2 connected components with 2 self-intersection points (Figure 2b)	2 connected components (Figure 2c)
$rM - rm < a < rm + rM$	2 connected components closed curves without self-intersection points (Figure 3a)	2 connected components closed curves without self-intersection points (Figure 3b)	2connected components closed curves without self-intersection points. Two circular arcs (Figure 3c)
$a = rm + rM$	two points: $(rM + rm, 0, 0)$ and $(-rm - rM, 0, 0)$ (Figure 4a)	two points: $(rM + rm, 0, 0)$ and $(-rm - rM, 0, 0)$ (Figure 4a)	two points: $(rM + rm, 0, 0)$ and $(-rm - rM, 0, 0)$ (Figure 4a)
$a > rm + rM$	empty set (Figure 4b)	empty set (Figure 4b)	empty set (Figure 4b)

Table 1. Cases $\mathcal{T}\bigcap\mathcal{H}_{(a,b)}$

Now, let us provide a detailed description of each of the cases.

4.1 When $a < rM - rm$, the intersection curve is composed by four connected components, as illustrated in Figure 1. As b approaches 0, the limit intersection curve is a curve composed by two circles (Figure 1c). On the other hand, as $b \to +\infty$, the hyperbolic cylinder tends towards two parallel planes, and the intersection curve becomes four coplanar circles (Figure 1b).

4.2 If $a = rM - rm$, the intersection curve has exactly two connected components, see Figure 2.

Analysing the cutcurve, two critical lines can be found, looking at the solutions of the system of equations:

$$S_0(x, y) = 0, \frac{\partial S_0}{\partial y}(x, y) = 0.$$

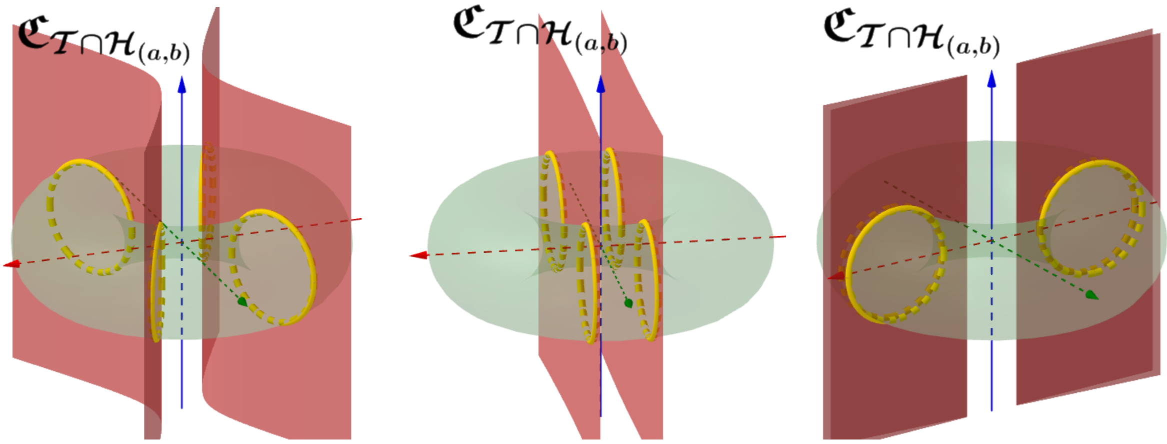

(a) $0 < b < \infty$ **(b)** $b \to +\infty$ **(c)** $b \to 0$

Figure 1. Cases where $a < rM - rm$.

These solutions can also be determined by the roots of:

$$\text{Resultant}\left(S_0(x,y), \frac{\partial \mathbf{S}_0}{\partial y}(x,y); y\right) = 4a^4b^2\,(a-x)\,(a+x)\,.$$

Critical points of the cutcurve are located on the lines $x = a$ and $x = -a$ (or $x = rM - rm$ and $x = rm - rM$). Furthermore, $(a, 0, 0)$ and $(-a, 0, 0)$ are common points to both surfaces. By computing the gradients of the polynomial functions associated with the respective implicit equations, at these points, we get:

$$\nabla\mathcal{H}\,(a,0,0) = \left(\frac{2}{a}, 0, 0\right) \qquad \nabla\mathcal{T}\,(a,0,0) = \left(4a^3 - 4rM^2a - 4a\,rm^2, 0, 0\right), \quad \text{and}$$

$$\nabla\mathcal{H}\,(-a,0,0) = \left(-\frac{2}{a}, 0, 0\right) \qquad \nabla\mathcal{T}\,(-a,0,0) = \left(-4a^3 + 4rM^2a + 4a\,rm^2, 0, 0\right)$$

Since these two pairs of vectors are collinear, the intersection points are points of tangential intersections.

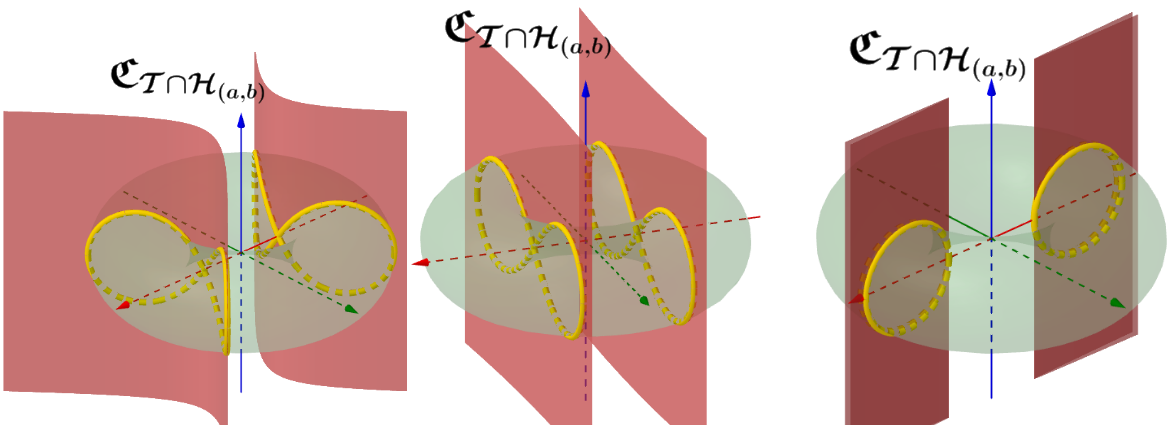

(a) $0 < b < \infty$ **(b)** $b \to +\infty$ **(c)** $b \to 0$

Figure 2. Cases where $a = rM - rm$.

Observe that when $b \to 0$, the intersection curve tends towards two circles (Figure 2c) and when $b \to +\infty$, the intersection curve tends towards a lemniscate (Figure 2c).

4.3 Let us assume now that $rM - rm < a < rm + rM$. In this case, the intersection curve is composed by two connected components closed curves without self-intersection points, see Figure 3.

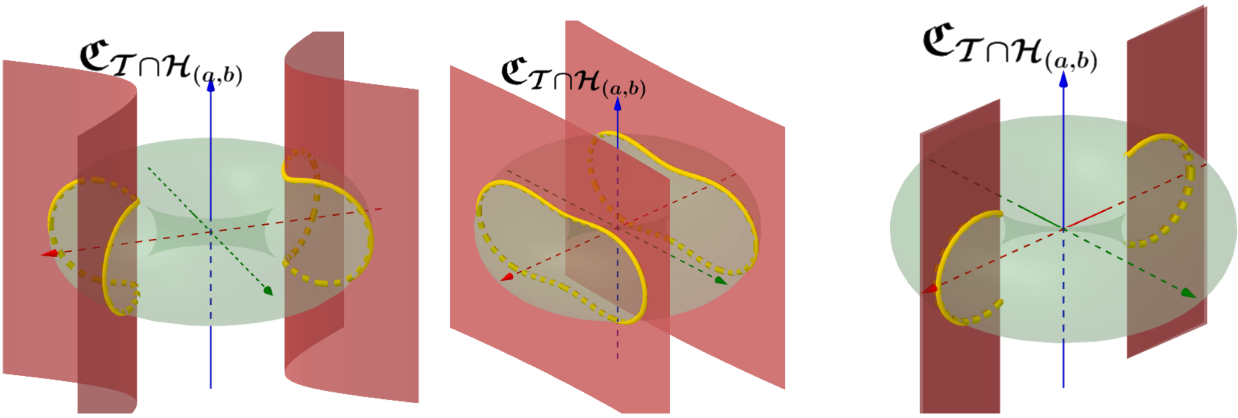

(a) $0 < b < \infty$ (b) $b \to +\infty$ (c) $b \to 0$

Figure 3. Cases where $rM - rm < a < rm + rM$.

When $b \to 0$ (Figure 3c) and $b \to +\infty$ (Figure 3b) the intersection remains defined by two connected components, which are two circular arcs when $b \to 0$.

4.4 If $a = rm + rM$, the points in the torus-hyperbolic cylinder intersection are the points with coordinates $(rM + rm, 0, 0)$ and $(-rm - rM, 0, 0)$ (Figure 4a).

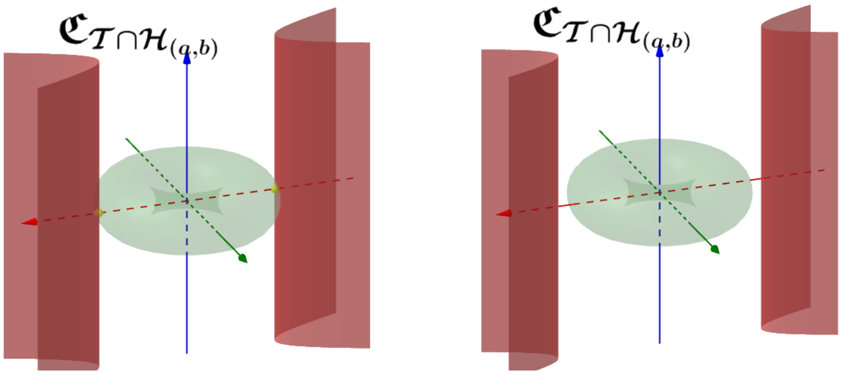

(a) $a = rm + rM$ (b) $a > rM + rm$

Figure 4. Cases where $a \geq rM + rm$.

4.5 If $a > rm + rM$ there is no intersection between the two surfaces, see Figure 4b.

To better understand the study we are carrying out, let us analyze a specific case that fits into case 4.1.

Example 1 Let $\mathcal{T}_{(O,4,1)}$ be a torus and $\mathcal{H}_{(2,1)}$ a hyperbolic cylinder with axis along the z-axis described by the equations:

$$\mathcal{T}_{(O,4,1)} : \left(x^2 + y^2 + z^2 + 15\right)^2 - 64x^2 - 64y^2 = 0 \quad \text{and} \quad \mathcal{H}_{(2,1)} : \frac{x^2}{4} - y^2 - 1 = 0.$$

The projection of the intersection curve in the xOy plane is given by the polynomial:

$$S_0 = -x^2 + 4y^2 + 4.$$

The cutcurve is contained within the region defined by $9 \leq x^2 + y^2 \leq 25$, and the intersection points between the cutcurve and silhouette curves are contained in the lines $x = \pm\frac{2\sqrt{130}}{5}$ and $x = \pm 2\sqrt{2}$, and thus, one branch of the cutcurve can be defined by

$$-x^2 + 4y^2 + 4 = 0 \wedge 2\sqrt{2} \leq x \leq \frac{2\sqrt{130}}{5} \wedge y \geq 0.$$

On the other hand, from the equation of torus and the equation of the branch defined above $\left(y=\sqrt{\frac{x^2}{4}-1}\right)$, we can conclude that the lifting of this branch can be made by using

$$z^2=\frac{\sqrt{-56-5x^2+16\sqrt{5x^2-4}}}{2}.$$

The parameterization of this branch can be defined by

$$\left(x,\sqrt{\frac{x^2}{4}-1},\pm\frac{\sqrt{-56-5x^2+16\sqrt{5x^2-4}}}{2}\right),\ x\in\left[2\sqrt{2},\frac{2\sqrt{130}}{5}\right].$$

The remaining connected components can be found by reflecting them in the xOz and yOz coordinate planes.

5. The case $\mathcal{T}\bigcap\mathcal{H}_{(b,c)}$

The curve in the xOy plane containing the projection of $\mathfrak{C}=\mathcal{T}\bigcap\mathcal{H}_{(b,c)}$ is defined by the squarefree polynomial:

$$\begin{aligned}S_0=b^4x^4+\left(b^2+c^2\right)^2y^4+2b^2\left(b^2+c^2\right)x^2y^2\\ -2\left(c^2+rM^2+rm^2\right)b^4x^2-2b^2\left(\left(c^2+rM^2+rm^2\right)b^2+c^2\left(c^2-rM^2+rm^2\right)\right)y^2\\ +\left(c^4+\left(-2rM^2+2rm^2\right)c^2+(rM+rm)^2(rM-rm)^2\right)b^4.\end{aligned}$$

S_0 is represented by $\mathcal{R}_{\mathcal{HT}}$, in figures 5 and 6.

In this case, the cutcurve, $\mathfrak{PC}_{\mathcal{T}\cap\mathcal{H}}$, is the part of this curve leaving in the admissible region and defined by

$$(rM-rm)^2\leq x^2+y^2\leq(rM+rm)^2\wedge(y\geq b\vee y\leq -b),$$

see figures 5 and 6. Note that $\mathfrak{PC}_{\mathcal{T}\cap\mathcal{H}}$ is the projection curve of the intersection of the two surfaces, $\mathfrak{C}_{\mathcal{T}\cap\mathcal{H}}$, in the plane xOy.

The intersection points of the cutcurve with the interior boundary of the admissible region, if any, are given by

$$\left(\pm\sqrt{(rM-rm)^2-b^2},\pm b,0\right),$$

$$\left(\pm\frac{\sqrt{-(b+rM-rm)(b-rM+rm)c^2+4b^2rM\ (rM-rm)}}{c},\pm\frac{\sqrt{c^2-4\,rM\ (rM-rm)}b}{c},0\right).$$

Regarding the intersection points of the cutcurve with the outer circle, their coordinates are given by

$$\left(\pm\sqrt{(rM+rm)^2-b^2},\pm b,0\right),$$

$$\left(\pm\frac{\sqrt{-(b+rM+rm)(b-rM-rm)c^2+4b^2rM\ (rM+rm)}}{c},\pm\frac{\sqrt{c^2-4\,rM\ (rM+rm)}b}{c},0\right).$$

The critical points of the cutcurve, $\mathfrak{PC}_{\mathcal{T}\cap\mathcal{H}}$, are located on the lines,

$$\begin{aligned}x=-rM-\sqrt{c^2+rm^2},x=-rM+\sqrt{c^2+rm^2},\\ x=\pm\frac{\sqrt{c^4+\left(b-\sqrt{(rM-rm)(rM+rm)}\right)\left(b+\sqrt{(rM-rm)(rM+rm)}\right)c^2+b^2rm^2}\,b}{\left(b^2+c^2\right)c},\\ x=rM-\sqrt{c^2+rm^2},\text{and } x=rM+\sqrt{c^2+rm^2}.\end{aligned}$$

The number of critical lines of $\mathcal{R}_{\mathcal{HT}}$ with interest to the behaviour of $\mathfrak{PC}_{\mathcal{T}\cap\mathcal{H}}$, depends on the values of the parameters b and c, and are crucial to identify the number of connected components of the intersection curves and the existence of critical points.

If the number of critical points of $\mathfrak{PC}_{\mathcal{T}\cap\mathcal{H}}$ is 4 or 6, then $\mathfrak{C}_{\mathcal{T}\cap\mathcal{H}}$ has 4 connected components none of them with self-intersection points (Figure 5).

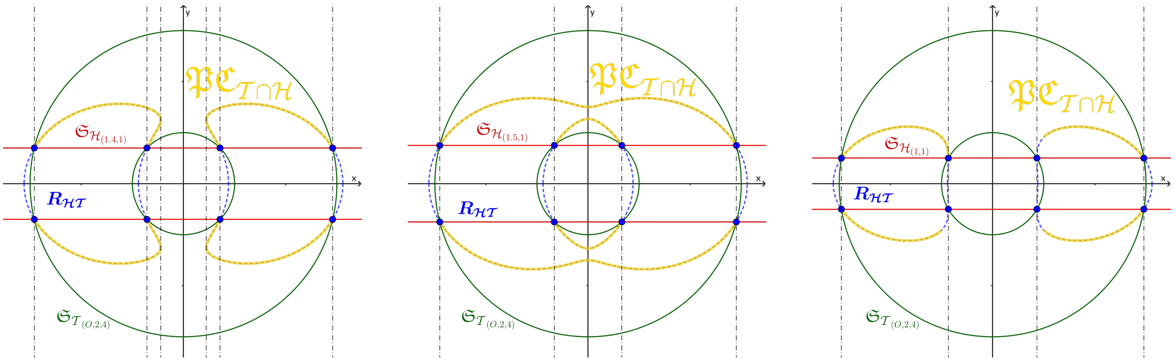

(a) $\mathcal{R}_{\mathcal{HT}}$ 6 critical lines, $\mathfrak{C}$ 4 connected components **(b)** $\mathcal{R}_{\mathcal{HT}}$ 4 critical lines, $\mathfrak{C}$ 4 connected components **(c)** $\mathcal{R}_{\mathcal{HT}}$ 4 critical lines, $\mathfrak{C}$ 4 connected components

Figure 5. Cases where $\mathfrak{C}_{\mathcal{T}\cap\mathcal{H}}$ do not have self-intersection points, examples based in $rM = 4 \wedge rm = 2$.

If the number of critical lines of $\mathfrak{PC}_{\mathcal{T}\cap\mathcal{H}}$ is 5 then $\mathfrak{C}_{\mathcal{T}\cap\mathcal{H}}$ has 2 connected components with two self-intersection points in each component, see Figure 6a.

If the number of critical lines of $\mathfrak{PC}_{\mathcal{T}\cap\mathcal{H}}$ is 3 then $\mathfrak{C}_{\mathcal{T}\cap\mathcal{H}}$ has either 2 *tangential* points and 2 connected components (Figure 6b); or 4 connected components where two of them are isolated points (Figure 6c).

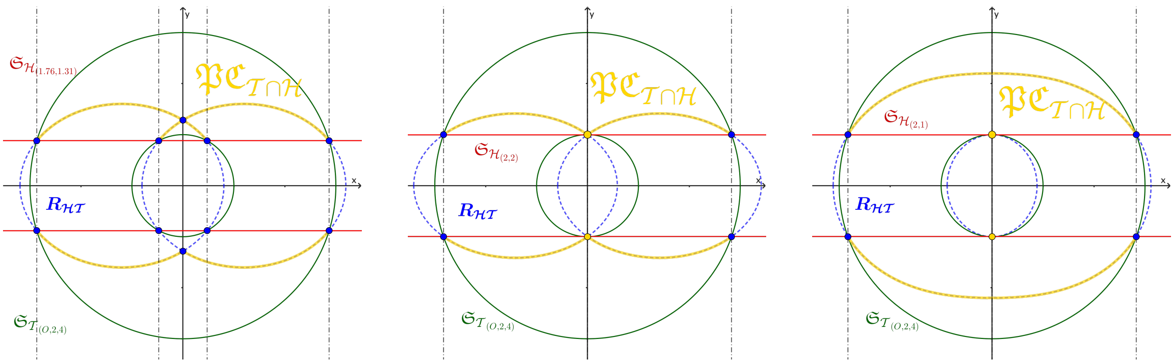

(a) $\mathcal{R}_{\mathcal{HT}}$ 5 critical lines, $\mathfrak{C}$ 2 self-intersection points **(b)** $\mathcal{R}_{\mathcal{HT}}$ 3 critical lines, $\mathfrak{C}$ 2 points connected components **(c)** $\mathcal{R}_{\mathcal{HT}}$ 3 critical lines, $\mathfrak{C}$ 2 tangential points

Figure 6. Cases where $\mathfrak{PC}_{\mathcal{T}\cap\mathcal{H}}$ has self-intersection points or singular points, examples based in $rM = 4 \wedge rm = 2$.

Let us now summarise all the possible scenarios for $\mathfrak{C}_{\mathcal{T}\cap\mathcal{H}}$, based on the variations of the real parameters b and c, and considering the following aspects: number of connected components; existence of self-intersection points; and cases of degeneracy. Special attention will be given to the cases in which the intersection curve approaches a planar curve.

The reason for presenting these findings in a way that differs from the one presented for $\mathcal{T}\cap\mathcal{H}(a,b)$ is the increased complexity associated with $\mathcal{T}\cap\mathcal{H}(b,c)$. As illustrated, for instance, in Figure 7d, the self-intersection points are located outside the equatorial plane of the Torus. In this specific case, studying the behavior and number of critical lines of the resultant within the admissible region, was crucial to classify the intersection curve. (Figure 6a).

Table 2 resumes all the cases to be considered having into account the variation of the parameters b and c. covering all cases.

Now we detail several cases according to the values of the parameters b and c.

5.1 $\mathcal{T}\cap\mathcal{H}_{(b,c)} = \emptyset$

For $c > 0 \wedge b > rM + rm$, the intersection $\mathcal{T}\cap\mathcal{H}_{(b,c)}$ is empty.

<table>
<tr><th></th><th>$0 < b < rM - rm$</th><th>$b = rM - rm$</th><th>$rM - rm < b < rM + rm$</th><th>$b = rM + rm$</th><th>$b > rM + rm$</th></tr>
<tr><td>$c \to 0$</td><td>If $c > b^*$ 4 connected components approach union of 4 arcs in the equatorial Torus circles
If $c < b^*$ 4 connected components collapsing in 2 connected components in union of planes $y = z$ and $y = -z$</td><td>2 connected components approach union of 2 equatorial Torus circles
see 5.5</td><td>2 connected components approach union of 2 arcs in the outer equatorial Torus circles, see 5.2</td><td rowspan="4">2 points
2 connected components
see 5.3</td><td rowspan="4">$\emptyset$
see 5.1</td></tr>
<tr><td>$0 < c < c^*$</td><td>4 connected components
$c < b^*$ resultant 4 critical lines
see 5.9
each with symmetry in xOy
$c > b^*$ resultant 6 critical lines
each with symmetry in planes xOy and yOz
see 5.8</td><td>4 connected components
2 of them are points
see 5.5
If $b = b^*$
2 connected components
each 2 self-intersection points outside $z = 0$
see 5.7</td><td rowspan="2">2 connected components without self-intersections points, see 5.4</td></tr>
<tr><td>$c \geq c^*$</td><td>4 connected components each with symmetry in xOy, see 5.10</td><td>2 connected components each 1 self-intersection point, see 5.6</td></tr>
<tr><td>$c \to \infty$</td><td>4 connected components approach union 4 circles, ray rm
see 5.10</td><td>2 connected components shaped like a lemniscate
see 5.6</td><td>2 connected components approach curves like ovals of Cassini
see 5.4</td></tr>
</table>

Notes:
$b^* = \frac{\sqrt{-(c^2+rm^2)(c^2-rM^2+rm^2)}\,c}{c^2+rm^2} \leq rM - rm$ and
$c^* = \sqrt{rm(rM - rm)}$

Table 2. Cases $\mathcal{T} \bigcap \mathcal{H}_{(b,c)}$

5.2 *$\mathcal{T} \cap \mathcal{H}_{(b,c)}$ is a planar curve with two connected components*
When c approaches $0, c \to 0$ and $rM - rm < b < rM + rm$, the hyperbolic cylinder degenerates in the union of two half-planes, and the intersection curve is the union of two circular arcs in the outer *equatorial* torus circle.

5.3 $\mathcal{T} \cap \mathcal{H}_{(b,c)} = \{(0, -b, 0), (0, b, 0)\}$
If $c > 0 \wedge b = rM + rm$, the intersection curve has two connected components, defined by the isolated points $(0, -(rM + rm), 0)$ and $(0, rM + rm, 0)$.

5.4 *$\mathcal{T} \cap \mathcal{H}_{(b,c)}$ is a curve with two connected components without self-intersections points*
If $c > 0 \wedge rM - rm < b < rM + rm$ the intersection curve has two connected components without self-intersections points. If $c \to \infty$ the components approach planar curves, a type of ovals of Cassini. See the example provided by $\mathfrak{C}_{\mathcal{T}_{(O,4,2)} \cap \mathcal{H}_{(3,3)}}$, illustrated in Figure 7a.

5.5 *$\mathcal{T} \cap \mathcal{H}_{(b,c)}$ is a curve with four connected components, two of which are isolated points*
If $0 < c < \sqrt{rMrm - rm^2} \wedge b = rM - rm$, the intersection curve has four connected components. Two of them are the points $(0, \pm(rM - rm), 0)$. If $c \to 0$ the intersection curve components approach to planar curves, two arcs in the outer *equatorial* torus circle. See, for instance, $\mathfrak{C}_{\mathcal{T}_{(O,4,2)} \cap \mathcal{H}_{(2,1)}}$, in Figure 7b.

5.6 *$\mathcal{T} \cap \mathcal{H}_{(b,c)}$ is a curve with two connected components, each of which with a point of self-intersection*
If $c \geq \sqrt{rM\,rm - rm^2} \wedge b = rM - rm$, the intersection curve has two connected components. Each component has one self-intersection point. The coordinates of these two points are $(0, \pm(rM - rm), 0)$. If $c \to \infty$, the intersection curve components approach planar curves shaped like a lemniscate. See as an example, the case $\mathfrak{C}_{\mathcal{T}_{(O,4,2)} \cap \mathcal{H}_{(2,4)}}$, illustrated in Figure 7c.

5.7 *$\mathcal{T} \cap \mathcal{H}_{(b,c)}$ is a curve with two connected components, with four self-intersection points (2 in each component)*
If $0 < c < \sqrt{rM\,rm - rm^2} \wedge b = \frac{\sqrt{-(c^2+rm^2)(c^2-rM^2+rm^2)}\,c}{c^2+rm^2}$, the intersection curve has two connected components, each one with two self-intersection points leaving outside the plane $z = 0$.
The coordinates of the intersection points are:
$$\left(0, \pm\frac{\sqrt{-(c^2+rm^2)(c^2-rM^2+rm^2)}}{crM^2}\sqrt{-\frac{(c^2-rM^2+rm^2)c^2rM^2}{c^2+rm^2}}, \pm\frac{c^2+rm^2}{crM^2}\sqrt{-\frac{c^2rM^2(c^2+rM\,rm+rm^2)(c^2-rM\,rm+rm^2)}{(c^2+rm^2)^2}}\right)$$
An example is provided by $\mathfrak{C}_{\mathcal{T}_{(O,4,2)} \cap \mathcal{H}_{(1,0.62)}}$, see Figure 7d.

5.8 *$\mathcal{T} \cap \mathcal{H}_{(b,c)}$ is a curve with four connected components*
If $0 < c < \sqrt{rM\,rm - rm^2} \wedge b > \frac{\sqrt{-(c^2+rm^2)(c^2-rM^2+rm^2)}c}{c^2+rm^2} \wedge b < rM - rm$, the intersection curve has four connected components. If $c \to 0$ each intersection curve component approaches a planar curve, arcs

in the outer and inner *equatorial* torus circle. This case occurs when the resultant has four critical lines, as illustrated above in Figure 6b. For a visualisation of this case, see the example provided by $\mathfrak{C}_{\mathcal{T}_{(O,4,2)} \cap \mathcal{H}_{(1,0.35)}}$, illustrated in Figure 7e.

5.9 $\mathcal{T} \cap \mathcal{H}_{(b,c)}$ *is a curve with four connected components*

If $0 < c < \sqrt{rM\,rm - rm^2} \wedge b < \frac{\sqrt{-(c^2+rm^2)(c^2-rM^2+rm^2)c}}{c^2+rm^2}$, the intersection curve has four connected components. It occurs when the resultant has six critical lines, as illustrated in Figure 6c. An example of this case is given by $\mathfrak{C}_{\mathcal{T}_{(O,4,2)} \cap \mathcal{H}_{(1.4,1)}}$, illustrated in Figure 7f.

5.10 $\mathcal{T} \cap \mathcal{H}_{(b,c)}$ with four connected components

If $c \geq \sqrt{rM\,rm - rm^2} \wedge 0 < b < rM - rm$, the intersection curve has four connected components. If $c \to \infty$, the hyperbolic cylinder approach the region defined by the union of the planes $y = -b$ and $y = b$, and so the intersection curve tends towards the union of four circles with ray rm. For visualise this case, see the example $\mathfrak{C}_{\mathcal{T}_{(O,4,2)} \cap \mathcal{H}_{(1,3)}}$ in Figure 7g.

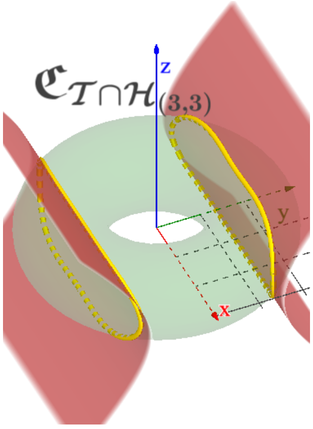

(a) $\mathfrak{P}\mathfrak{C}_{\mathcal{T}\cap\mathcal{H}}$ 4 critical lines, $\mathfrak{C}$ 2 connected components

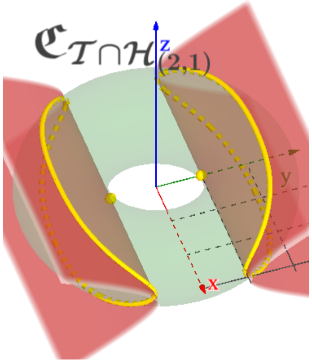

(b) $\mathfrak{P}\mathfrak{C}_{\mathcal{T}\cap\mathcal{H}}$ 4 critical lines, $\mathfrak{C}$ 2 points, 4 connected components

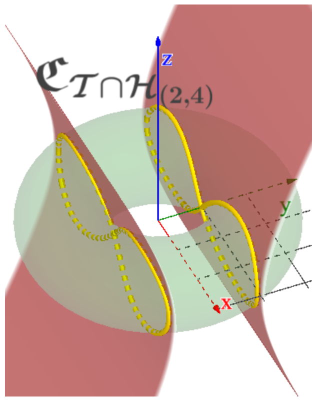

(c) $\mathfrak{P}\mathfrak{C}_{\mathcal{T}\cap\mathcal{H}}$ 4 critical lines, $\mathfrak{C}$ 2 tangential points, 2 connected components

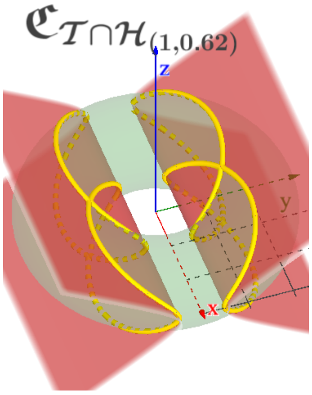

(d) $\mathfrak{P}\mathfrak{C}_{\mathcal{T}\cap\mathcal{H}}$ 5 critical lines, $\mathfrak{C}$ 2 auto intersection points, 2 connected components

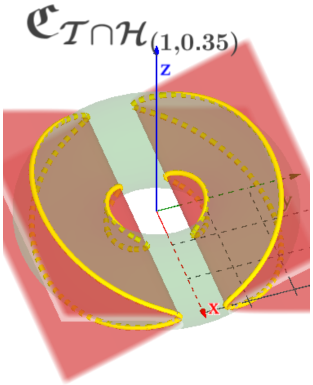

(e) $\mathfrak{P}\mathfrak{C}_{\mathcal{T}\cap\mathcal{H}}$ 4 critical lines, $\mathfrak{C}$ 4 connected components

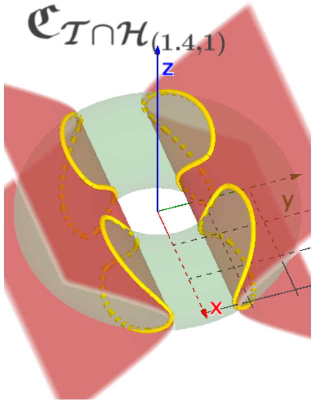

(f) $\mathfrak{P}\mathfrak{C}_{\mathcal{T}\cap\mathcal{H}}$ 6 critical lines, $\mathfrak{C}$ 4 connected components

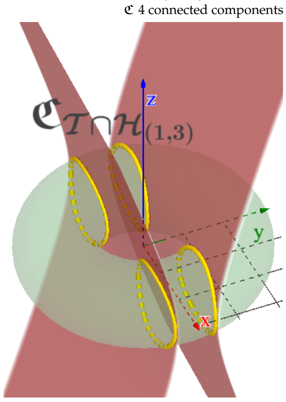

(g) $\mathfrak{P}\mathfrak{C}_{\mathcal{T}\cap\mathcal{H}}$ 4 critical lines, $\mathfrak{C}$ 4 connected components

Figure 7. The $\mathfrak{C}_{\mathcal{T}\cap\mathcal{H}_{(b,c)}}$, examples based in $rM = 4 \wedge rm = 2$

Next, we analyse in more detail what happens with $\mathcal{T}_{(O,4,2)}\ cap \mathcal{H}_{(1,1)}$ which fits in the case 5.9.

Example 2 Let $\mathcal{T}_{(O,4,2)}$ be a torus and $\mathcal{H}_{(1,1)}$ a hyperbolic cylinder with axis along the x-axis described by the equations:

$$\mathcal{T}_{(O,4,2)} : \left(x^2+y^2+z^2+12\right)^2 - 64(x^2-y^2) = 0 \quad \text{and} \quad \mathcal{H}_{(1,2)} : y^2 - \frac{z^2}{4} - 1 = 0.$$

The projection of the intersection curve in the xOy plane is given by the polynomial:

$$S_0 = x^4 + 25\ y^4 + 10\ x^2\ y^2 - 48\ x^2 + 16\ y^2 + 64.$$

The cutcurve is contained within the region defined by $4 \leq x^2+y^2 \leq 36 \wedge (y \leq -1 \vee y \geq 1)$, and the intersection points between the cutcurve and silhouette curves are contained in the lines $x = \pm\sqrt{35}$ and

$x = \pm\sqrt{3}$. Thus, one branch of the cutcurve can be defined by

$$x^4 + 25\,y^4 + 10\,x^2\,y^2 - 48\,x^2 + 16\,y^2 + 64 = 0 \wedge \sqrt{3} \leq x \leq \sqrt{35} \wedge y \geq 0.$$

On the other hand, from the torus equation and the equation of the branch given above $\left(y = \sqrt{\frac{z^2}{4} + 1}\right)$, we can conclude that the lifting of this branch can be obtained by using

$$z^2 = \frac{-20\,x^2 + 64\,\sqrt{5\,x^2 - 6} - 132}{25}.$$

Thus $y = \frac{\sqrt{-5\,x^2 + 16\,\sqrt{5\,x^2-6} - 8}}{5}$, and the parameterization of this branch can be defined by

$$\left(x, \frac{\sqrt{-5\,x^2 + 16\,\sqrt{5\,x^2 - 6} - 8}}{5}, \pm\frac{2\sqrt{-5\,x^2 + 16\,\sqrt{5\,x^2 - 6} - 33}}{5}\right), x \in \left[\sqrt{3}, \sqrt{35}\right].$$

The other connected components can be found by reflecting them in the xOz and yOz coordinate planes.

6. Conclusions

Through a detailed and accurate analysis of the number of connected components and self-intersecting points, we have successfully classified the families of curves resulting from the intersection of a hyperbolic cylinder and a Torus, sharing a common center. This classification has been achieved by combining various methodologies and techniques and was inspired by previous works on the intersection of quadrics with a torus.

With this study, we have adapted and presented new relevant processes to obtain the findings reported here, contributing to a broader understanding of the intersection of algebraic surfaces. The combination and exploration of these processes enhanced the knowledge of the geometric and topological properties of the intersection curves.

We intend to expand the scope of this work, considering the intersection of a torus with an elliptical cylinder and a parabolic cylinder. These scenarios will probably also present challenges and complexities requiring a scrupulous examination. By applying or adapting the processes developed here, we anticipate gaining further insights into the behavior and characteristics of the intersecting curves of algebraic surfaces.

Funding

This research was supported by the Center for Research and Development in Mathematics and Applications (CIDMA) through the Portuguese Foundation for Science and Technology (FCT - Fundação para a Ciência e a Tecnologia), references UIDB/04106/2020 (`https://doi.org/10.54499/UIDB/04106/2020`) and UIDP/04106/2020 (`https://doi.org/10.54499/UIDP/04106/2020`); The Centre for Research and Innovation in Education (inED), through the FCT - Fundação para a Ciência e a Tecnologia, I.P., under the scope of the project UIDP/05198/2020 (`https://doi.org/10.54499/UIDP/05198/2020`); and Department of Mathematics of University of Coimbra (`https://doi.org/10.54499/UIDB/00324/2020`).

Availability of data and materials

Not applicable.

Competing interests

The authors declare that they have no competing interests.

Author's contributions

All authors contributed equally to the writing of this paper. All authors read and approved the final manuscript.

References

[1] Breda, A. M., Trocado, A., Dos Santos, J. M.: *The intersection curve of an ellipsoid with a torus sharing the same center.* In: Proceedings of the 20th International Conference on Geometry and Graphics (ICGG2022), 127-137. Springer International Publishing (2023). https://doi.org/10.1007/978-3-031-13588-0_11

[2] Breda, A. M., Trocado, A., Dos Santos, J. M.: *Torus and quadrics intersection using GeoGebra.* In: Proceedings of the 19th International Conference on Geometry and Graphics (ICGG2020), 484-493. Springer International Publishing (2021). https://doi.org/10.1007/978-3-030-63403-2_43

[3] Gonzalez-Vega, L., Trocado, A.: *Using maple to compute the intersection curve of two quadrics: Improving the intersectplot command.* Maple in Mathematics Education and Research, 92-100. Springer International Publishing (2020). https://doi.org/10.1007/978-3-030-41258-6_7

[4] Gonzalez-Vega, L., Trocado, A.: *Tools for analyzing the intersection curve between two quadrics through projection and lifting.* Journal of Computational and Applied Mathematics, **393**, 113522 (2021). https://doi.org/10.1016/j.cam.2021.113522

[5] Kim, K., Kim, M., Oh, K.: *Torus/sphere intersection based on a configuration space approach.* Graphical Models and Image Processing, **60** (1), 77–92 (1998). https://doi.org/10.1006/gmip.1997.0451

[6] Pironti, A., Walker, M.: *Fusion, tokamaks, and plasma control: an introduction and tutorial.* IEEE Control Systems Magazine, **25** (5), 30–43 (2005). https://10.0.4.85/MCS.2005.1512794

[7] Gonzalez-Vega, L., Trocado, A., Dos Santos, J. M.: *Intersecting two quadrics with GeoGebra.* Algebraic Informatics, 237-248. Springer International Publishing (2019). https://doi.org/10.1007/978-3-030-21363-3_20

[8] Gonzalez-Vega, L.: *A subresultant theory for multivariate polynomials.* In: Proceedings of the International Symposium on Symbolic and Algebraic Computation (ISSAC'91), 79-85. ACM (1991).

Affiliations

Ana Maria Reis D'Azevedo Breda
Address: University of Aveiro, Dept. of Portugal, Campus Universitário de Santiago 3810-193, Aveiro-Portugal.
e-mail: ambreda@ua.pt
ORCID ID:0000-0001-7076-707X

Alexandre Emanuel Batista da Silva Trocado
Address: Instituto GeoGebra Portugal, R. Dr. Roberto Frias 602, 4200-465, Porto-Portugal.
e-mail: mail@alexandretrocado.com,
ORCID ID:0000-0001-5589-8100

José Manuel Dos Santos Dos Santos
Address: University of Coimbra, Dept. of Mathematics, Largo D. Dinis, 3000-143, Coimbra-Portugal.
e-mail: dossantos@uc.pt
ORCID ID:0000-0002-6830-6503